

# OH-Si complex in hydrogenated n-type $\beta$ -Ga<sub>2</sub>O<sub>3</sub>:Si

Cite as: Appl. Phys. Lett. **119**, 062109 (2021); <https://doi.org/10.1063/5.0059769>

Submitted: 11 June 2021 . Accepted: 29 July 2021 . Published Online: 13 August 2021

Andrew Venzie, Amanda Portoff,  Chaker Fares,  Michael Stavola,  W. Beall Fowler,  Fan Ren, and  Stephen J. Pearton



View Online



Export Citation



CrossMark

## ARTICLES YOU MAY BE INTERESTED IN

[Thermal stability of epitaxial  \$\alpha\$ -Ga<sub>2</sub>O<sub>3</sub> and \(Al,Ga\)<sub>2</sub>O<sub>3</sub> layers on m-plane sapphire](#)

Applied Physics Letters **119**, 062102 (2021); <https://doi.org/10.1063/5.0064278>

[High electron mobility and low noise quantum point contacts in an ultra-shallow all-epitaxial metal gate GaAs/Al<sub>x</sub>Ga<sub>1-x</sub>As heterostructure](#)

Applied Physics Letters **119**, 063105 (2021); <https://doi.org/10.1063/5.0053816>

[Deep level study of chlorine-based dry etched  \$\beta\$ -Ga<sub>2</sub>O<sub>3</sub>](#)

Journal of Applied Physics **130**, 025701 (2021); <https://doi.org/10.1063/5.0050416>



**A new approach to low-level measurements of nanostructures**

Read our technical note

[Download Now](#)



# OH-Si complex in hydrogenated n-type $\beta$ -Ga<sub>2</sub>O<sub>3</sub>:Si

Cite as: Appl. Phys. Lett. **119**, 062109 (2021); doi: 10.1063/5.0059769

Submitted: 11 June 2021 · Accepted: 29 July 2021 ·

Published Online: 13 August 2021



View Online



Export Citation



CrossMark

Andrew Venzie,<sup>1</sup> Amanda Portoff,<sup>1</sup> Chaker Fares,<sup>2</sup> Michael Stavola,<sup>1,a)</sup> W. Beall Fowler,<sup>1</sup> Fan Ren,<sup>2</sup> and Stephen J. Pearton<sup>3</sup>

## AFFILIATIONS

<sup>1</sup>Department of Physics, Lehigh University, Bethlehem, Pennsylvania 18015, USA

<sup>2</sup>Department of Chemical Engineering, University of Florida, Gainesville, Florida 32611, USA

<sup>3</sup>Department of Materials Science and Engineering, University of Florida, Gainesville, Florida 32611, USA

<sup>a)</sup> Author to whom correspondence should be addressed: [michael.stavola@Lehigh.edu](mailto:michael.stavola@Lehigh.edu)

## ABSTRACT

Si is an n-type dopant in Ga<sub>2</sub>O<sub>3</sub> that can be intentionally or unintentionally introduced. The results of Secondary Ion Mass Spectrometry, Hall effect, and infrared absorption experiments show that the hydrogen plasma exposure of Si-doped Ga<sub>2</sub>O<sub>3</sub> leads to the formation of complexes containing Si and H and the passivation of n-type conductivity. The Si-H (D) complex gives rise to an O-H (D) vibrational line at 3477.6 (2577.8) cm<sup>-1</sup> and is shown to contain a single H (or D) atom. The direction of the transition moment of this defect has been investigated to provide structure-sensitive information. Theory suggests possible structures for an OH-Si complex that is consistent with its observed vibrational properties.

Published under an exclusive license by AIP Publishing. <https://doi.org/10.1063/5.0059769>

$\beta$ -Ga<sub>2</sub>O<sub>3</sub> is attracting much recent attention as an ultra-wide bandgap semiconductor that shows great promise for high-power, deep UV, and extreme environment applications.<sup>1–6</sup> Hydrogen can give rise to n-type conductivity in a variety of transparent conducting oxides,<sup>7–9</sup> and  $\beta$ -Ga<sub>2</sub>O<sub>3</sub> is no exception where several hydrogen centers have been reported to be shallow donors.<sup>10,11</sup> Therefore, it seems counterintuitive that hydrogen plasma exposure could introduce H into Ga<sub>2</sub>O<sub>3</sub> that passivates the Si<sub>Ga</sub> center that is also a shallow donor.<sup>10,12,13</sup> Nonetheless, it has been recently reported that hydrogen plasma exposure compensates or passivates Si<sub>Ga</sub> shallow donors in micrometer-thick layers of Ga<sub>2</sub>O<sub>3</sub> grown by hydride-vapor-phase epitaxy and that these effects are anisotropic.<sup>14–16</sup> In the present work, the introduction of hydrogen into a Si-doped layer by hydrogen plasma exposure has been investigated by Secondary Ion Mass Spectrometry (SIMS) and vibrational spectroscopy.<sup>17,18</sup> We show that H (and D) form complexes with Si<sub>Ga</sub> in Ga<sub>2</sub>O<sub>3</sub> leading to its passivation.

There is a growing body of information about H in Ga<sub>2</sub>O<sub>3</sub> and its interactions with other defects that affect conductivity.<sup>11,13,19–27</sup> The V<sub>Ga(1)</sub> center in Ga<sub>2</sub>O<sub>3</sub> gives rise to a deep triple acceptor and has shifted configurations that have low formation energies.<sup>28–32</sup> Theory and positron annihilation spectroscopy suggest that V<sub>Ga</sub> deep acceptors compensate n-type shallow donors.<sup>28,33,34</sup> V<sub>Ga(1)</sub>-nH complexes are predicted to have even lower formation energies than V<sub>Ga(1)</sub> and also act as deep acceptors that could compensate shallow donors.<sup>22,28</sup> The V<sub>Ga(1)</sub>-2H center has been found to be the dominant hydrogen-

containing center in undoped Ga<sub>2</sub>O<sub>3</sub> hydrogenated either by annealing in an H<sub>2</sub> ambient or by the implantation of protons.<sup>19–21</sup> (There are two shifted configurations of V<sub>Ga(1)</sub> that can trap H atoms.<sup>22,28,29</sup> The shifted configuration of V<sub>Ga(1)</sub> predicted by Kyrtos *et al.*<sup>29</sup> is the hydrogen trap that gives rise to the most stable V<sub>Ga(1)</sub>-2H center that has been observed by vibrational spectroscopy.<sup>19</sup> The implantation of protons into Ga<sub>2</sub>O<sub>3</sub> has been found to give rise to a resistive layer whose defects are suggested to interact with the implanted H upon annealing to restore the layer's conductivity.<sup>23</sup> Another recent study reports that the controlled introduction of H into Ga<sub>2</sub>O<sub>3</sub> can give rise to both n-type and p-type behaviors.<sup>11</sup>

Samples for our studies were prepared from Ga<sub>2</sub>O<sub>3</sub> epitaxial layers that were purchased from Novel Crystal Technology and had been grown by molecular-beam-epitaxy to be 0.5  $\mu$ m thick and doped with Si to a concentration of  $2 \times 10^{18}$  cm<sup>-3</sup>. The (010) semi-insulating Ga<sub>2</sub>O<sub>3</sub> substrate was doped with Fe. Samples were treated in H- or D-plasmas for 60 min at a nominal temperature of 250 °C and were characterized with Hall effect measurements and SIMS (EAG Laboratories). Detection limits for SIMS for Si and D were reported to be  $5 \times 10^{15}$  and  $3 \times 10^{15}$  cm<sup>-3</sup>, respectively.<sup>35</sup>

IR absorption spectra were measured with a Nicolet iS50 Fourier transform infrared spectrometer equipped with a CaF<sub>2</sub> beam splitter and an InSb detector. The probing light was incident normal to the face of the sample, and the polarization was analyzed with a wire grid polarizer that was placed after the sample. Samples were cooled to

77 K for our measurements with a Helitran continuous-flow cryostat. Annealing treatments to probe the thermal stabilities of defects were performed in a tube furnace with a flowing Ar ambient.

Following a treatment in a D-plasma, a  $\text{Ga}_2\text{O}_3$  sample was characterized by SIMS. Results for the concentration profiles of Si and D are shown in Fig. 1. The depth profile for Si shows a concentration of  $[\text{Si}] = 3 \times 10^{18} \text{ cm}^{-3}$  for the  $0.5 \mu\text{m}$ -thick epitaxial layer. The D profile shows a plateau with a concentration  $[\text{D}] > 5 \times 10^{18} \text{ cm}^{-3}$  throughout most of the thickness of the Si-doped epilayer. The D concentration then drops to near  $4 \times 10^{17} \text{ cm}^{-3}$  beyond a depth of  $0.5 \mu\text{m}$ , i.e., in the Fe-doped semi-insulating substrate. The formation of a plateau in the D-profile that follows the dopant concentration profile is typical of the compensation or passivation of the dopant impurity in the layer.<sup>36</sup> Similar profiles were observed by Polyakov *et al.*<sup>15</sup> for Si-doped  $\text{Ga}_2\text{O}_3$  layers ( $n \approx 10^{17} \text{ cm}^{-3}$ ) treated in a “harsh” D-plasma.

Prior to treatment in an H-plasma, Hall measurements found a carrier concentration of  $3.0 \times 10^{18} \text{ cm}^{-3}$ , a resistivity of  $2.9 \times 10^{-2} \Omega \text{ cm}$ , and a mobility of  $70 \text{ cm}^2/\text{Vs}$  for our  $\text{Ga}_2\text{O}_3$ :Si epitaxial sample. Following a treatment in an H-plasma, the carrier concentration was reduced to  $1.2 \times 10^{18} \text{ cm}^{-3}$  and the resistivity and mobility were increased to  $5.4 \times 10^{-2} \Omega \text{ cm}$  and  $96 \text{ cm}^2/\text{Vs}$ , respectively. These results for the decrease in the electrical activity of the n-dopant in the layer along with an increase in the Hall mobility provides further evidence for the compensation and/or passivation of  $\text{Si}_{\text{Ga}}$  by hydrogen.

Infrared absorption spectra are shown in Figs. 2 for  $\text{Ga}_2\text{O}_3$ :Si epilayers treated in D and H plasmas. [The D spectrum (c) was measured for a piece of the same D-treated sample whose SIMS profiles are shown in Fig. 1.] The frequencies of the O-D (O-H) lines are  $2577.8$  ( $3477.6$ ) and  $2584.6$  ( $3489.8$ )  $\text{cm}^{-1}$ . These two lines have also been observed in bulk  $\text{Ga}_2\text{O}_3$  samples annealed in at a  $\text{D}_2$  ambient but have different relative intensities in the different samples, indicating that they arise from different defects. The line at  $2577.8$  ( $3477.6$ )  $\text{cm}^{-1}$  is stronger for the Si-doped epilayer shown here, while the line at  $2584.6$  ( $3489.8$ )  $\text{cm}^{-1}$  is stronger for a deuterated bulk substrate deliberately doped with Fe (inset to Fig. 2). Both Si and Fe are adventitious impurities in  $\text{Ga}_2\text{O}_3$  with typical concentrations near  $10^{17} \text{ cm}^{-3}$  (see, for example, Refs. 37 and 38), and the substrate for our Si-doped epitaxial

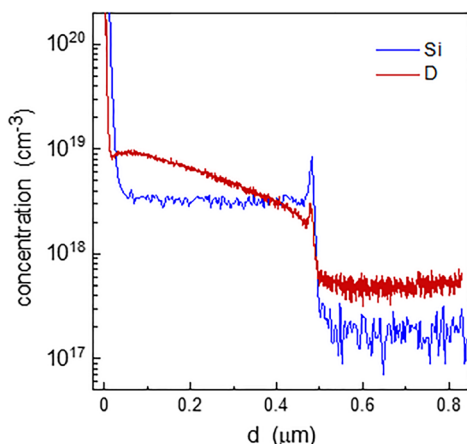


FIG. 1. SIMS profiles for Si and D in a Si-doped  $\text{Ga}_2\text{O}_3$  epitaxial layer grown by MBE that was subsequently treated in a D-plasma.

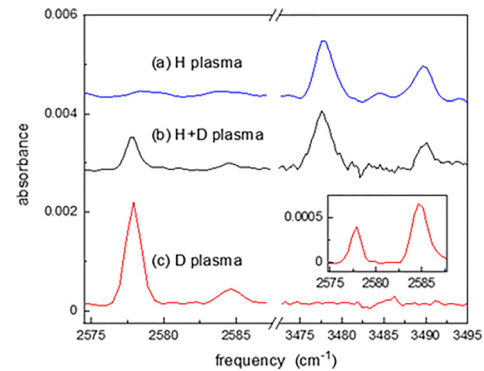


FIG. 2. IR spectra (77 K) of Si-doped  $\text{Ga}_2\text{O}_3$  epitaxial layers treated for 30 min ( $250^\circ\text{C}$ ) in (a) an H plasma, (b) a plasma containing H and D, and (c) a D plasma. The inset shows a spectrum for an Fe-doped  $\text{Ga}_2\text{O}_3$  substrate annealed in a  $\text{D}_2$  ambient at  $1000^\circ\text{C}$ .

layer is intentionally doped with Fe so it is not surprising that we see hydrogen centers associated with both of these impurities in our samples. We assign the  $2577.8$  and  $3477.6 \text{ cm}^{-1}$  lines to Si-D and Si-H complexes, respectively, because they are dominant in spectra for samples deliberately doped with Si. We assign the  $2584.6$  and  $3489.8 \text{ cm}^{-1}$  lines to Fe-D and Fe-H complexes because they are dominant in spectra for samples deliberately doped with Fe. The appearance of distinct lines associated with Si and Fe in  $\text{Ga}_2\text{O}_3$  indicates the close proximity of these impurities to the vibrating H (or D) atom and is consistent with the formation of passivated complexes rather than a compensation process for which the impurity atom and H could be more distant. In the following, we focus on the lines at  $2577.8$  and  $3477.6 \text{ cm}^{-1}$  and the hydrogen passivation of the Si donor in  $\text{Ga}_2\text{O}_3$ . Investigations of the Fe-D (H) complex are in progress in our laboratory.

Equation (1) yields an estimate of the concentration,  $N$ , of Si-D centers in our samples from the integrated absorbance for the IR line at  $2577.8 \text{ cm}^{-1}$  shown in the lower spectrum in Fig. 2 and a calibration determined in Ref. 24 (an effective charge of  $q = 0.47e$ ) for O-D centers in  $\text{Ga}_2\text{O}_3$ . This equation<sup>17</sup> is written in CGS units to be consistent with the absorption coefficient and frequency  $\bar{\nu}$  in units  $\text{cm}^{-1}$ . Here,  $m$  is the mass of the oscillating impurity,  $n$  is the refractive index,  $c$  is the speed of light, and  $l$  is the thickness of the absorbing layer.

$$N = (2.303 m n c^2 / l \pi q^2) \int A(\bar{\nu}) d\bar{\nu}. \quad (1)$$

The concentration of Si-D centers in the  $0.5 \mu\text{m}$  Si-doped epitaxial layer treated in a  $\text{D}_2$  plasma is estimated to be  $3.8 \times 10^{18} \text{ cm}^{-3}$ . We take the agreement of this result with the concentration of Si in the epitaxial layer determined by SIMS and Hall effect to be fortuitous, given that the errors in defect concentrations calculated from IR intensities can easily be a factor of 2 or more. Nonetheless, this result shows that the intensity of the  $2577.8 \text{ cm}^{-1}$  IR line reported here is consistent with most or a significant fraction of the Si in the epitaxial layer being involved in the defect giving rise to that line and provides further support for the assignment of the  $2577.8 \text{ cm}^{-1}$  line to a Si-D complex.

O-H and O-D centers containing one or two H or D atoms have been observed in  $\text{Ga}_2\text{O}_3$  by others.<sup>19,25,26</sup> Centers that contain two H or D atoms can be identified from the characteristic IR spectra that

occur for samples that contain both H and D where a fraction of the defects that are produced contain both H and D atoms. Spectrum (b) in Fig. 2 was measured for a sample treated in a plasma that contained both H and D and shows both the O-H and O-D lines at  $3477.6$  and  $2577.8\text{ cm}^{-1}$ , respectively, in the same sample with a relative intensity of 4:1. When spectrum (b) in Fig. 2 for the sample containing both H and D is compared with spectra (a) and (c) in the same figure, there is no sign of a line splitting, broadening, or shift that would be characteristic of a defect that contained both hydrogen isotopes. These results are consistent with Si-H and Si-D complexes that contain a single H or D atom.

The results of annealing experiments that probe the thermal stabilities of the  $2577.8$  and  $2584.6\text{ cm}^{-1}$  lines due to Si-D and Fe-D complexes are shown in Fig. 3. IR absorbance spectra were measured for a sample initially treated in a  $\text{D}_2$  plasma and then subsequently annealed (30 min) at successively higher temperatures. Spectra were measured for two polarization angles, one near the maximum for the  $2577.8\text{ cm}^{-1}$  absorption and the second at  $90^\circ$  with respect to this angle.

Both the  $2577.8$  and  $2584.6\text{ cm}^{-1}$  lines were produced by the plasma treatment. Upon annealing at  $100^\circ\text{C}$ , the  $2577.8\text{ cm}^{-1}$  line increased in intensity by 70%, suggesting that a portion of the D introduced by the plasma treatment remained present in a form available to interact with impurities in the sample. ( $\text{D}_2$  and  $\text{D}_\text{O}$  centers are candidates for a form of D produced by a D-plasma treatment that does not give rise to an observable O-D vibrational mode.) The  $2577.8\text{ cm}^{-1}$  line is annealed away at  $400^\circ\text{C}$ . As the  $2577.8\text{ cm}^{-1}$  line decreased in strength at  $350^\circ\text{C}$ , the intensity of the  $2584.6\text{ cm}^{-1}$  line increased before it finally disappeared at  $450^\circ\text{C}$ . The different annealing behaviors of the  $2577.8$  and  $2584.6\text{ cm}^{-1}$  lines confirm that they arise from two different defects.

When the  $2577.8$  and  $2584.6\text{ cm}^{-1}$  lines are completely annealed away at  $450^\circ\text{C}$ , the  $2546.4\text{ cm}^{-1}$  line assigned previously to the  $\text{V}_{\text{Ga}(1)}\text{-2D}$  complex appears for the polarization direction oriented  $90^\circ$  with respect to the direction giving strong absorption for the  $2577.8$  and  $2584.6\text{ cm}^{-1}$  lines. These results confirm that the  $2577.8$  and  $2584.6\text{ cm}^{-1}$  lines have transition moment directions in the a-c plane roughly perpendicular to that of the  $\text{V}_{\text{Ga}(1)}\text{-2D}$  center whose transition moment is  $\approx 15^\circ$  clockwise from the  $[102]$  direction.<sup>39</sup>

The directions of the transition moments for O-H (O-D) centers in  $\text{Ga}_2\text{O}_3$  provide structure-sensitive information about the defects. There are two types of Si-D complexes whose O-D transition

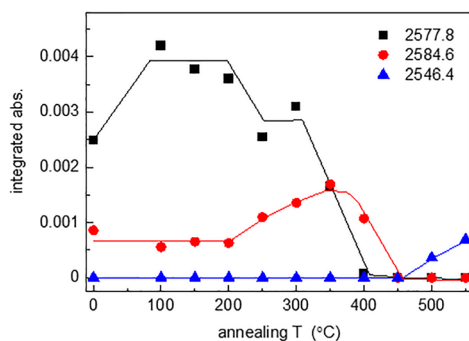


**FIG. 3.** Annealing behavior of a Si-doped  $\text{Ga}_2\text{O}_3$  epitaxial layer treated in a  $\text{D}_2$  plasma whose spectrum prior to annealing is shown in Fig. 2(c). The lines are drawn to guide the eye.

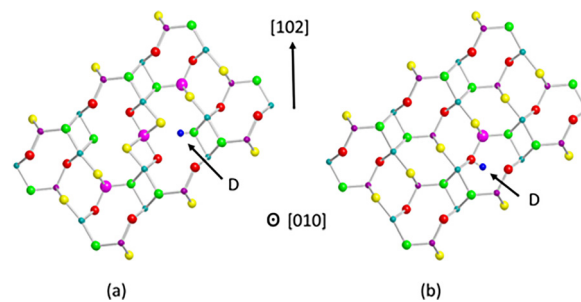


**FIG. 4.** Possible structures of the defect associated with the  $2577.8\text{ O-D}$  line. (a) shifted  $\text{Ga}(1)$  vacancy with a trapped D and three candidate Si substitutional sites. (b) D trapped next to a Si substituted for a  $\text{Ga}(1)$ . The inequivalent atomic sites are color coded as follows:  $\text{Ga}(1)$ , purple;  $\text{Ga}(2)$ , dark green;  $\text{O}(1)$ , red;  $\text{O}(2)$ , yellow,  $\text{O}(3)$ , light green; and Si, pink. These figures were constructed using MOLDRAW<sup>41</sup> and POV-Ray.<sup>42</sup>

moments within the a-c plane could approximately satisfy the observed O-D moment direction for the  $2577.8\text{ cm}^{-1}$  line. Fig. 4(a) shows a  $\text{Ga}(1)$  vacancy shifted as predicted by Varley *et al.*<sup>28</sup> A single H is trapped at an unsaturated  $\text{O}(3)$ , while three potential sites for a Si substituted for a  $\text{Ga}(1)$  are shown. We have theoretically investigated this situation using the CRYSTAL17 code<sup>40</sup> with computational parameters used in previous calculations<sup>19–22</sup> and find only small variations of the transition moment direction from that perpendicular to the  $(-201)$  plane. This direction is then  $\approx 75^\circ$  from the  $\approx 15^\circ$  moment for the  $\text{V}_{\text{Ga}(1)}\text{-2D}$  center.

Figure 4(b) shows a H trapped at an  $\text{O}(1)$  site next to a Si that is substituted for a  $\text{Ga}(1)$ . Our calculations find that in this case the transition moment direction is  $\approx 125^\circ$  clockwise from the  $[102]$  direction. It is, thus,  $\approx 110^\circ$  from the transition moment for the  $\text{V}_{\text{Ga}(1)}\text{-2D}$  center.

Our O-H (O-D) spectra and their polarization dependence are consistent with both of the structures shown in Fig. 4 and do not allow us to rule out either of these possible assignments for the  $2577.8\text{ cm}^{-1}$  line.

In conclusion, the introduction of H into Si doped  $\text{Ga}_2\text{O}_3$  leads to the formation of an OH-Si complex and a reduction of n-type conductivity. Theory suggests possible structures for an OH-Si complex that are consistent with the observed vibrational properties.

The work at Lehigh University was supported by NSF under Grant No. DMR 1901563 (James Edgar). The work at UF was sponsored by Department of the Defense, Defense Threat Reduction Agency, No. HDTRA1-17-1-011, monitored by J. Calkins, DTRA Interaction of Ionizing Radiation with Matter University Research Alliance, HDTRA1-19-S-0004 (Jacob Calkins), and also by NSF DMR 1856662 (James Edgar). Portions of this research were conducted with research computing resources provided by Lehigh University.

## DATA AVAILABILITY

The data that support the findings of this study are available from the corresponding author upon reasonable request.

## REFERENCES

- <sup>1</sup>M. Higashiwaki, A. Kuramata, H. Murakami, and Y. Kumagai, *J. Phys. D: Appl. Phys.* **50**, 333002 (2017).
- <sup>2</sup>M. Higashiwaki and G. H. Jessen, *Appl. Phys. Lett.* **112**, 060401 (2018).



- <sup>3</sup>S. J. Pearton, J. Yang, P. H. Cary, F. Ren, J. Kim, M. J. Tadjer, and M. A. Mastro, *Appl. Phys. Rev.* **5**, 011301 (2018).
- <sup>4</sup>J. Zhang, J. Shi, D.-C. Qi, L. Chen, and K. H. L. Zhang, “Recent progress on the electronic structure, defect, and doping properties of Ga<sub>2</sub>O<sub>3</sub>,” *APL Mater.* **8**, 020906 (2020).
- <sup>5</sup>*Ga2O3: Technology, Devices and Applications*, edited by S. J. Pearton, F. Ren, and M. Mastro (Elsevier, Amsterdam, 2018).
- <sup>6</sup>*Wide Bandgap Semiconductor-based Electronics*, edited by F. Ren and S. J. Pearton (Institute of Physics Publishing, Bristol, 2020).
- <sup>7</sup>P. D. C. King and T. D. Veal, *J. Phys.: Condens. Matter* **23**, 334214 (2011).
- <sup>8</sup>M. D. McCluskey, M. C. Tarun, and S. T. Teklemichael, *J. Mater. Res.* **27**, 2190 (2012).
- <sup>9</sup>M. Stavola, W. B. Fowler, Y. Qin, P. Weiser, and S. J. Pearton, in *Ga2O3, Technology, Devices and Applications*, edited by S. J. Pearton, F. Ren, and M. Mastro (Elsevier, Amsterdam, 2018), Chap. 9, p. 191.
- <sup>10</sup>J. B. Varley, J. R. Weber, A. Janotti, and C. G. Van de Walle, *Appl. Phys. Lett.* **97**, 142106 (2010).
- <sup>11</sup>M. M. Islam, M. O. Liedke, d Winarski, M. Butterling, A. Wagner, P. Hoseman, Y. Wang, B. Uberuaga, and F. A. Selim, *Sci. Rep.* **10**, 6134 (2020).
- <sup>12</sup>E. G. Villora, K. Shimamura, Y. Koshikawa, T. Ujiie, and K. Aoki, *Appl. Phys. Lett.* **92**, 202120 (2008).
- <sup>13</sup>M. D. McCluskey, *J. Appl. Phys.* **127**, 101101 (2020).
- <sup>14</sup>A. Y. Polyakov, I.-H. Lee, N. B. Smirnov, E. B. Yakimon, I. V. Shchemerov, A. V. Chernykh, A. I. Kochkova, A. A. Vasilev, A. S. Shiko, F. Ren, P. H. Carey, and S. J. Pearton, *Appl. Phys. Lett.* **115**, 032101 (2019).
- <sup>15</sup>A. Y. Polyakov, I.-H. Lee, N. B. Smirnov, E. B. Yakimon, I. V. Shchemerov, A. V. Chernykh, A. I. Kochkova, A. A. Vasilev, A. S. Shiko, P. H. Carey, F. Ren, and S. J. Pearton, *ECS J. Solid State Sci. Technol.* **8**, P661 (2019).
- <sup>16</sup>A. Y. Polyakov, I.-H. Lee, A. Miakonkikh, A. V. Chernykh, N. B. Smirnov, I. V. Shchemerov, A. I. Kochkova, A. A. Vasilev, and S. J. Pearton, *J. Appl. Phys.* **127**, 175702 (2020).
- <sup>17</sup>M. Stavola, in *Identification of Defects in Semiconductors*, edited by M. Stavola (Academic, Boston, 1998), Chap. 3, Vol. 51B, p. 153.
- <sup>18</sup>M. Stavola and W. B. Fowler, *J. Appl. Phys.* **123**, 161561 (2018).
- <sup>19</sup>P. Weiser, M. Stavola, W. B. Fowler, and Y. Qin, *Appl. Phys. Lett.* **112**, 232104 (2018).
- <sup>20</sup>Y. Qin, M. Stavola, W. B. Fowler, P. Weiser, and S. J. Pearton, *ECS J. Solid State Sci. Technol.* **8**, Q3103 (2019).
- <sup>21</sup>A. Portoff, A. Venzie, Y. Qin, M. Stavola, W. B. Fowler, and S. J. Pearton, *ECS J. Solid State Sci. Technol.* **9**, 125006 (2020).
- <sup>22</sup>W. B. Fowler, M. Stavola, Y. Qin, and P. Weiser, *Appl. Phys. Lett.* **117**, 142101 (2020).
- <sup>23</sup>V. M. Reinertsen, P. M. Weiser, V. K. Frodason, M. E. Bathen, L. Vines, and K. M. Johansen, *Appl. Phys. Lett.* **117**, 232106 (2020).
- <sup>24</sup>A. Karjalainen, P. Weiser, I. Makkanen, V. Reinertsen, L. Vines, and F. Tuomisto, *J. Appl. Phys.* **129**, 165702 (2021).
- <sup>25</sup>J. R. Ritter, J. Huso, P. T. Dickens, J. B. Varley, K. G. Lynn, and M. D. McCluskey, *Appl. Phys. Lett.* **113**, 052101 (2018).
- <sup>26</sup>J. R. Ritter, K. G. Lynn, and M. D. McCluskey, *J. Appl. Phys.* **126**, 225705 (2019).
- <sup>27</sup>N. H. Nickel and K. Geilert, *J. Appl. Phys.* **129**, 195704 (2021).
- <sup>28</sup>J. B. Varley, H. Peelaers, A. Janotti, and C. G. Van de Walle, *J. Phys.: Condens. Matter* **23**, 334212 (2011).
- <sup>29</sup>A. Krytsos, M. Matsubara, and E. Bellotti, *Phys. Rev. B* **95**, 245202 (2017).
- <sup>30</sup>H. J. von Bardeleben, S. Zhou, U. Gerstmann, D. Skachkov, W. R. L. Lambrecht, Q. Ho, and P. Deak, *APL Mater.* **7**, 022521 (2019).
- <sup>31</sup>D. Skachkov, W. R. L. Lambrecht, H. J. von Bardeleben, U. Gerstmann, Q. D. Ho, and P. Deak, *J. Appl. Phys.* **125**, 185701 (2019).
- <sup>32</sup>J. M. Johnson, Z. Chen, J. B. Varley, C. M. Jackson, E. Farzana, Z. Zhang, A. R. Arehart, H.-L. Huang, A. Genc, S. A. Ringel, C. G. Van de Walle, D. A. Muller, and J. Hwang, *Phys. Rev. X* **9**, 041027 (2019).
- <sup>33</sup>E. Kohonen, F. Tuomisto, D. Gogova, G. Wagner, M. Baldini, Z. Galazka, R. Schewski, and M. Albrecht, *Appl. Phys. Lett.* **106**, 242103 (2015).
- <sup>34</sup>S. K. Swain, M. H. Weber, J. Jesenovec, M. Saleh, K. G. Lynn, and J. S. McCloy, *Phys. Rev. Appl.* **15**, 054010 (2021).
- <sup>35</sup>EAG Laboratories, private communication (Dec. 18, 2020).
- <sup>36</sup>*Hydrogen in Crystalline Semiconductors*, edited by S. J. Pearton, J. W. Corbett, and M. Stavola (Springer-Verlag, Heidelberg, 1992).
- <sup>37</sup>A. Kuramata, K. Koshi, S. Watanabe, Y. Yamaoka, T. Masui, and S. Yamakoshi, *Proc. SPIE* **10533**, 105330E (2018).
- <sup>38</sup>M. E. Ingebrigtsen, J. B. Varley, A. Y. Kuznetsov, B. G. Svensson, G. Alfieri, M. Mihaila, J. Badstübner, and L. Vines, “Iron and intrinsic deep level states in Ga<sub>2</sub>O<sub>3</sub>,” *Appl. Phys. Lett.* **112**, 042104 (2018).
- <sup>39</sup>A. Portoff, A. Venzie, M. Stavola, W. B. Fowler, and S. Pearton, *J. Appl. Phys.* **127**, 055702 (2020).
- <sup>40</sup>R. Dovesi, A. Erba, R. Orlando, C. M. Zicovich-Wilson, B. Civalieri, L. Maschio, M. Rérat, S. Casassa, J. Baima, S. Salustro, and B. Kirtman, “Quantum-mechanical condensed matter simulations with CRYSTAL,” *WIREs Comput. Mol. Sci.* **8**, e1360 (2018).
- <sup>41</sup>See P. Ugliengo, <http://moldraw.unito.it> for “MOLDRAW” (2006).
- <sup>42</sup>See <http://povray.org> for “POV-Ray.”